

## Aqueous Gold Sols of Rod-Shaped Particles

Bianca M. I. van der Zande,<sup>\*,†,‡</sup> Marcel R. Böhmer,<sup>†</sup> Lambertus G. J. Fokkink,<sup>†</sup> and Christian Schönenberger<sup>†,§</sup>

Philips Research Laboratories, Prof. Holstlaan 4, 5656 AA Eindhoven, The Netherlands, and Van't Hoff Laboratory for Physical and Colloid Chemistry, Utrecht University, Padualaan 8, 3584 CH Utrecht, The Netherlands

Received: June 27, 1996<sup>⊗</sup>

Aqueous dispersions of rodlike gold particles are obtained by electrodeposition in nanopores of anodized alumina attached to a conductive support followed by dissolution of the alumina and stabilization of the rods with poly(vinylpyrrolidone). The obtained sol of monodisperse gold rods is examined by electron microscopy and visible (VIS) and near-infrared (NIR) spectroscopy. In the VIS/NIR absorption spectra two absorption maxima are present. With increasing aspect ratio, the maximum around 520 nm shifts to shorter wavelength, while the other maximum shifts into the near-infrared regime, which is in agreement with theoretical predictions.

### Introduction

Recently, the interest in aqueous model systems of anisotropic particles has grown. Anisotropic particles dispersed in liquids show interesting properties, because of their behavior in external fields and in concentrated systems. In external fields these colloidal particles have the ability to align with the field, resulting in changes in the optical properties or the rheological behavior of the suspensions. In concentrated systems, phase separation resulting in a phase with an orientational order is observed.<sup>1,2</sup> However, suspensions of anisotropic particles often exhibit a high degree of heterodispersity,<sup>3–5</sup> which complicates their colloid chemical behavior.

By using electrodeposition in nanoporous aluminum oxide, monodisperse colloidal metal rods of controllable aspect ratio can be obtained.<sup>6</sup> In this Letter, we present a method to release the rods grown in nanoporous alumina to obtain an aqueous sol. We decided to study aqueous sols of gold rods, because firstly the stabilization of gold colloids<sup>7–10</sup> is well documented and, secondly, the spectroscopic properties of both sols of spherical gold particles<sup>11–13</sup> and gold rods embedded in an alumina membrane<sup>6,14–16</sup> are known. The aqueous dispersions are examined by transmission electron microscopy (TEM) and visible/near-infrared (VIS/NIR) spectroscopy. Colloidal rods can also be obtained by electrodeposition in nanopores of polycarbonate membranes,<sup>17–19</sup> and, in principle, rods of different metals can be synthesized.<sup>20</sup>

### Electrodeposition in Nanoporous Aluminum Oxide

Porous aluminum oxide was obtained by anodization of aluminum.<sup>21–23</sup> The porous aluminum oxide membrane has a thickness of 1.5  $\mu\text{m}$ , a pore density of about  $8 \times 10^{14} \text{ m}^{-2}$ , and an average pore diameter equal to 12 nm. The electrodeposition of gold was preceded by electrodeposition of a small amount of copper.<sup>6,24,25</sup> Copper can be selectively dissolved,<sup>26</sup> which enables the release of the gold rods from the support. The length of the gold particles can be easily varied by changing the deposition time,<sup>6</sup> while the pore diameter (and therefore the

particle diameter) can be widened by chemical dissolution of the aluminum oxide.<sup>21,24</sup>

### Release of the Synthesized Rods Resulting in Aqueous Colloidal Dispersions

To release the rods, the aluminum oxide was dissolved in a 1.25 M NaOH solution.<sup>6,21,24,27,28</sup> Subsequently, the copper, which fixes the gold rods to the substrate, was selectively dissolved<sup>26</sup> resulting in rods lying flat on the substrate. Finally, 10 such samples were collected and dispersed into 2 mL of demineralized water by ultrasonification. As the rods stay on the surface after dissolution of the copper, a dispersion medium other than water can in principle be chosen at this stage of sol preparation.

To be able to disperse the rods, a suitable stabilizer has to be chosen, which is facilitated by the extensive documentation on classical gold sol stabilization.<sup>7–10</sup> Addition of citrate<sup>8</sup> did not result in a stable sol. Large flocs were observed immediately after release from the substrate. For the high ionic strength of the system (due to the dissolution of alumina and copper), citrate adsorption does not lead to stabilization because the electrostatic repulsion is too weak. However, by using uncharged polymers, steric stabilization can be achieved.<sup>7,9,29,30</sup> We found that addition of 4 g/L poly(vinylpyrrolidone) (PVP,  $M = 40\,000$ , Fluka) to the sodium hydroxide solution resulted in a stable sol. It was found that the VIS/NIR absorption was constant over a few weeks for diluted  $L/d = 4$  rod dispersions, while the VIS/NIR absorption of  $L/d = 13$  rod dispersions was constant for a few days. This is a strong indication that a colloidally stable system has indeed been obtained.

Figure 1 shows electron microscopy pictures of the gold rods synthesized by the present method. Figure 1a shows that gold rods directly deposited into the pores (without copper) all have the same length. Parts a and b of Figure 1 show the dispersed gold rods with aspect ratio  $L/d = 4$  and 13, respectively. The rod diameter is the same for both samples:  $d = 12$  nm. However, some polydispersity ( $\pm 25\%$ ) in the rod length is present. The procedure followed of mixing of 10 samples may account for the observed polydispersity. Some of the rods have side branches or surface irregularities due to the shape of the pores, and some of the particles are aggregated. These aggregates may have been formed during drying.

<sup>†</sup> Philips Research Laboratories.

<sup>‡</sup> Utrecht University.

<sup>§</sup> Present address: Institute for Physics, University Basel, Klingelbergstr. 82, CH-4056 Basel, Switzerland.

<sup>⊗</sup> Abstract published in *Advance ACS Abstracts*, December 15, 1996.

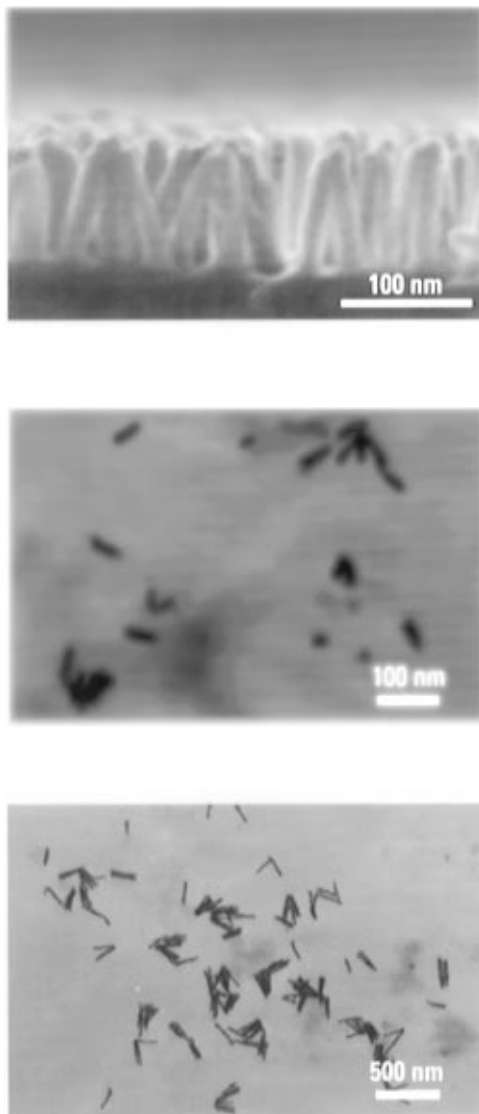


**Figure 1.** Electron microscopy photographs of dispersed gold rods. Part a (top) shows gold rods grown in porous aluminum oxide membranes performing gold deposition directly on the platinum pore bottom. In this particular case, the diameter of the pore was widened using 1 % (w/w)  $\text{H}_3\text{PO}_4$ <sup>21,24</sup> for 5 min resulting in a pore diameter of 18 nm. Photograph 1a was obtained with a field emission gun scanning electron microscope (Philips XL30 FEG-SEM, operated at 25 kV). Parts b (middle) and c (bottom) obtained with a transmission electron microscope (Philips CM30-TEM, operated at 300 kV) show the dispersion with rods of  $L/d = 4$  and the dispersion with rods of  $L/d = 13$ , respectively. The samples were prepared by dipping standard TEM substrates (Formvar) into the dispersion.

### VIS/NIR Spectroscopy

The dispersions of monodisperse gold rods were studied with VIS/NIR spectroscopy and compared with a sol consisting of spherical particles, synthesized following Frens,<sup>8</sup> except that 0.1 mL of 180 g/L K90-PVP (Fluka,  $M = 360\,000$ ) is added. The diameter of the spheres ( $d = 12$  nm) is equal to the rod diameter. The VIS/NIR absorption spectra recorded on a Perkin-Elmer UV/VIS/NIR Lambda 9 double-beam spectrophotometer are given in Figure 2.

The dispersion of the short rods was of a greyish color, while that of the long rods was pink. As is shown in Figure 2, the optical properties of the dispersion indeed change markedly with aspect ratio. Instead of a single adsorption maximum for the spherical gold sol, two maxima exist for the rods. The maximum for the rods around  $\lambda = 530$  nm is attributed to the

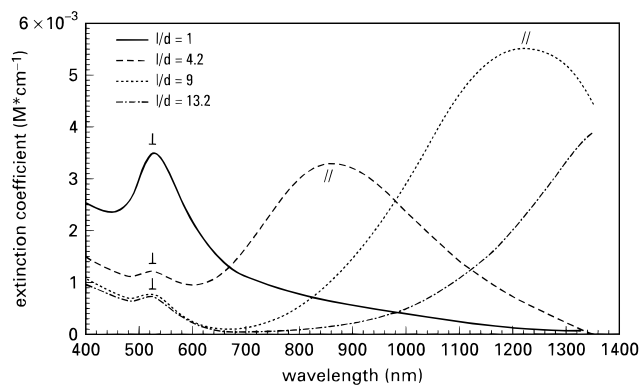


**Figure 2.** Normalized experimental VIS/NIR absorption spectra of rod dispersions with aspect ratio  $L/d = 1$  (spherical gold sol),  $L/d = 4$ ,  $L/d = 9$ , and  $L/d = 13$ .

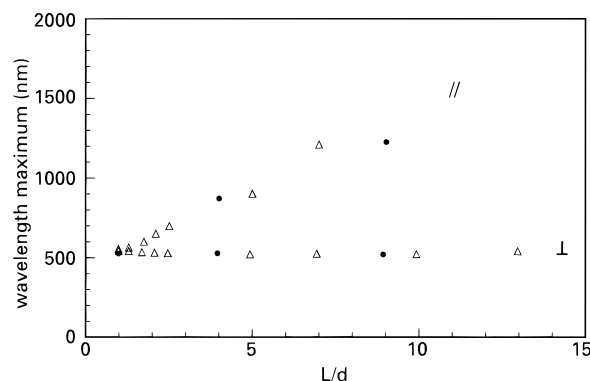


**Figure 3.** Experimental (●) and calculated<sup>31</sup> (Δ) positions of plasmon absorption maxima of the longitudinal resonance (||) and of plasmon absorption maxima of the transverse resonance (⊥).

transverse plasmon resonance (⊥);<sup>14,31,32</sup> The particles are oriented parallel to the incident wave vector of light, and the plasmon oscillates perpendicular to the long axis. With increasing aspect ratio, this maximum shifts to slightly shorter wavelengths and is damped. This shift to shorter wavelengths with increasing aspect ratio was also observed by Foss et al.,<sup>14</sup> who studied the optical properties of gold rods embedded in a porous aluminum oxide membrane (i.e. with the rods oriented parallel to the incident wave vector of light). In the case of a random orientation of the rods with respect to the incident wave vector of light, an additional optical effect caused by anisotropy of the particles is present. This, far more pronounced, second peak in the near infrared is attributed to the longitudinal plasmon resonance (||);<sup>31–33</sup> The particles are oriented with their long axis perpendicular to the incident wave vector of light, and the plasmon oscillates parallel to the long axis. This second absorption maximum shows an extreme shift to longer wavelengths with increasing aspect ratio. The absorption behavior of small prolate spheroids of silver randomly embedded in gelatin as studied by Skillman<sup>34</sup> is similar to the absorption behavior of aqueous dispersions of gold rods.

In Figure 3 the positions of the absorption maxima are given as a function of the aspect ratio ( $L/d$ ); Figure 3 also shows the results of a model calculations by Lebedeva.<sup>31</sup> The extinction coefficient in ref 31 was separately obtained for the case in which the incident wave vector of light was parallel and perpendicular to the long axis of the ellipsoidal gold particle. The observed shift of the longitudinal resonance is extreme compared to the shift of the transverse maximum and agrees with the calculations. However, the small transverse shift slightly deviates from Lebedeva's calculations. Our results for the transverse resonance for rods with  $d = 12$  nm are between

the experimental results of Foss et al.<sup>14</sup> for rods with  $d > 12$  nm embedded in an alumina membrane and the theoretical calculations for rods for which only the aspect ratio  $L/d$  is specified.<sup>14,31</sup> Because of the dependence of the transverse resonance on the aspect ratio as well as on the diameter, we conclude that our transverse resonance results are consistent with the results presented in refs 14 and 31.

### Conclusion

A stable colloidal aqueous system of gold rods is synthesized by using electrodeposition in nanopores of porous aluminum oxide followed by dissolution of the membrane, stabilization of the rods with PVP, and detachment of the substrate. The optical behavior of aqueous dispersions of the rods depends strongly on the aspect ratio of the particles. Due to the anisotropy, the absorption spectrum of randomly oriented colloidal gold rods comprises a longitudinal and a transverse resonance contribution at wavelengths that are in agreement with theoretical predictions. The higher the degree of anisotropy, the further into the infrared the maximum of the longitudinal resonance is shifted. The maximum of the transverse resonance is shifted to shorter wavelengths.

**Acknowledgment.** The authors thank C. Geenen, M. Krijn, and A. Staals (Philips Research Laboratories, Eindhoven) for making the electronmicrographs. Prof. Dr. H. N. W. Lekkerkerker and Prof. Dr. A. P. Philipse (Van't Hoff laboratory for Physical and Colloid Chemistry, Utrecht University) are thanked for stimulating discussions. This work is part of the research program of the Foundation for Fundamental Research on Matter (FOM) with financial support from the Netherlands Organization for Scientific Research (NWO).

### References and Notes

- (1) Vrooge, G. J.; Lekkerkerker, H. N. W. *Rep. Prog. Phys.* **1992**, *55*, 1241.
- (2) Buitenhuis, J.; Donselaar, L. N.; Buining, P. A.; Stroobants, A.; Lekkerkerker, H. N. W. *J. Colloid Interface Sci.* **1995**, *175*, 46.
- (3) Esumi, K.; Matsuhisa, K.; Torigue, K. *Langmuir* **1995**, *11*, 3285.
- (4) Tanori, J.; Pileni, M. P. *Adv. Mater.* **1995**, *7*, 862.
- (5) Buining, P. A.; Pathmamanoharan, C.; Jansen, J. B. H.; Lekkerkerker, H. N. W. *J. Am. Ceram. Soc.* **1991**, *74*, 1303.
- (6) Foss, C. A.; Hornyak, G. L.; Tierney, M. J.; Martin, C. R. *J. Phys. Chem.* **1992**, *96*, 9001.
- (7) Hirai, H. *J. Macromol. Sci., Chem.* **1979**, *13* (5), 633.
- (8) Frens, G. *Nature (London), Phys. Sci.* **1973**, *241*, 20.
- (9) Thiele, H.; Kavallik, J. *Kolloid Z. Z. Polym.* **1969**, *234*, 1017.
- (10) Handley, D. A. *Colloidal Gold: Principles, Methods, and Applications*; Hayat, M. A., Ed.; Academic Press Inc.: San Diego, CA, 1989; Vol. 1, Chapter 2.
- (11) Henglein, A. *J. Phys. Chem.* **1993**, *97*, 5457.
- (12) Doremus, R. H. *J. Chem. Phys.* **1964**, *40*, 2389.
- (13) Mulvaney, P.; Giersig, M.; Henglein, A. *J. Phys. Chem.* **1992**, *96*, 10419.
- (14) Foss, C. A.; Hornyak, G. L.; Stockert, J. A.; Martin, C. R. *J. Phys. Chem.* **1994**, *98*, 2963.
- (15) Preston, C. K.; Moskovits, M. *J. Phys. Chem.* **1988**, *92*, 2957.
- (16) Preston, C. K.; Moskovits, M. *J. Phys. Chem.* **1993**, *97*, 8495.
- (17) Whitney, T. M.; Jiang, J. S.; Searson, P. C.; Chien, C. L. *Science* **1993**, *261*, 1316.
- (18) Martin, C. R. *Science* **1994**, *266*, 1961.
- (19) We found that a colloidal dispersion of gold rods can also be obtained, starting from polycarbonate membranes as a template. At one side the polycarbonate membrane was covered with a copper electrode which enables the electrodeposition of gold. After electrodeposition of gold, the copper electrode is selectively dissolved.<sup>26</sup> Subsequently, the polycarbonate membrane in which the gold rods are embedded is dissolved in 2 mL of dichloromethane ( $T = 40$  °C) containing 0.026 g/mL poly(vinylpyridine) (P2VP) as a stabilizer resulting in a stable dispersion of gold rods in dichloromethane.
- (20) Goad, D. G. W.; Moskovits, M. *J. Appl. Phys.* **1978**, *49*, 2929.
- (21) Tsuya, N.; Tokushima, T.; Shiraki, M.; Wakui, Y.; Saito, Y.; Nakumara, H.; Katsumata, Y. *IEEE Trans. Magn.* **1987**, *23*, 53.
- (22) Diggle, J. W.; Downie, T. C.; Goulding, C. W. *Chem. Rev.* **1969**, *69*, 365.
- (23) Squares of size  $14 \times 14$  mm cut from Si wafers served as a support. These supports were successively covered with 10 nm titanium, 100 nm platinum, and 1  $\mu$ m aluminum by vacuum vapor deposition. The titanium ensures a good adhesion of the platinum on silicon. The aluminum is converted into porous aluminum oxide by anodization at a constant voltage of 15 V in 15 v/v % H<sub>2</sub>SO<sub>4</sub>.
- (24) Arai, K. I.; Kang, W.; Ishiyama, K. *IEEE Trans. Magn.* **1991**, *26*, 4906.
- (25) Copper deposition takes place for 100 s at a constant voltage of  $-0.05$  V vs a standard calomel electrode (SCE) applied by a PAR 273A (EG&G Princeton Applied Research) potentiostat/galvanostat using a 0.01 M copper(II) sulfate solution (pH between 1 and 2). The length of the copper rods is about 30 nm. An extra electrodeposition step was applied in a 0.01 M H<sub>2</sub>SO<sub>4</sub> solution and a constant voltage of  $-0.2$  V vs SCE to deposit copper ions, which might still be present in the nanopores after 100 s deposition. This extra electrodeposition step was necessary to get gold rods with controllable aspect ratio. Subsequently, gold is deposited on top of the copper at a constant voltage of  $-1.00$  V vs SCE (Figure 1c). A 0.32 M gold(I) cyanide electrolyte solution, containing 0.26 M citric acid and 0.65 M KOH, with a final pH between 5 and 6 is used. The typical current density was about  $70 \mu\text{A cm}^{-2}$  membrane area. The total membrane area is  $0.65 \text{ cm}^2$ ; the total pore area (actual deposition area) is estimated to be 10% of this area.
- (26) The copper is selectively dissolved using a 1:100 diluted copper etching solution, with a composition of 25 mL/L 98% H<sub>2</sub>SO<sub>4</sub>, 175 mL/L 30% H<sub>2</sub>O<sub>2</sub>, and a few drops of 85% H<sub>3</sub>PO<sub>4</sub>, for 30 min.
- (27) Pontifex, G. H.; Zhang, P.; Wang, Z.; Haslett, T. L.; Almawlawi, D.; Moskovits, M. *J. Phys. Chem.* **1991**, *95*, 9989.
- (28) Tsuya, N.; Tokushima, T.; Wakui, Y.; Saito, Y.; Nakamura, H.; Harada, Y. *IEEE Trans. Magn.* **1988**, *24*, 2661.
- (29) Hoogsteen, W.; Fokkink, L. G. J. *J. Colloid Interface Sci.* **1995**, *175*, 12.
- (30) Huang, H. H.; Ni, X. P.; Loy, G. L.; Chew, C. H.; Tan, K. L.; Loh, F. C.; Deng, J. F.; Xu, G. Q. *Langmuir* **1996**, *12*, 909.
- (31) Lebedeva, V. N.; Distler, G. I. *Opt. Spectrosc.* **1967**, *23*, 527.
- (32) Blatchford, C. G.; Campbell, J. R.; Creighton, J. A. *Surf. Sci.* **1982**, *120*, 435.
- (33) Creighton, J. A.; Eadon, D. G. *J. Chem. Soc., Faraday Trans.* **1991**, *87*, 3883.
- (34) Skillman, D. C.; Berry, C. R. *J. Chem. Phys.* **1968**, *48*, 3297.